

Supporting Information for:

# Chemically Controlled Crystal Growth of $(\text{CH}_3\text{NH}_3)_2\text{AgInBr}_6$

*Thao T. Tran,<sup>§</sup> Michael A. Quintero,<sup>§,⊥</sup> Kathryn E. Arpino,<sup>§,||</sup> Zachary A. Kelly,<sup>§</sup> Jessica R.*

*Panella,<sup>§</sup> Xiaoping Wang,<sup>ζ,\*</sup> and Tyrel M. McQueen<sup>§,‡,\*</sup>*

<sup>§</sup>Department of Chemistry, Department of Physics and Astronomy, Institute for Quantum Matter, Johns Hopkins University, Baltimore, MD 21218, United States

<sup>ζ</sup> Neutron Scattering Division, Spallation Neutron Source, Oak Ridge National Laboratory, Oak Ridge, TN 39831, United States

<sup>‡</sup> Department of Materials Science and Engineering, Johns Hopkins University, Baltimore, MD 21218, United States

CORRESPONDING AUTHOR EMAIL ADDRESS: [wangx@ornl.gov](mailto:wangx@ornl.gov) and [mcqueen@jhu.edu](mailto:mcqueen@jhu.edu)

<b>Table of contents</b>	
<b>Experiments</b>	<b>3</b>
<b>Figure S1.</b> Powder XRD	<b>6</b>
<b>Figure S2.</b> Jobs analysis for chemical compositions of activated complex	<b>7</b>
<b>Figure S3.</b> Rietveld refinements of the laboratory PXRD pattern	<b>8</b>
<b>Figure S4.</b> IR spectra of $(MA)_2AgInBr_6$	<b>9</b>
<b>Figure S5.</b> UV spectra of $(MA)_2AgInBr_6$	<b>10</b>
<b>Figure S6.</b> TGA/DSC measurements of $(MA)_2AgInBr_6$	<b>11</b>
<b>Figure S7.</b> PXRD of residue after TGA/DSC measurements	<b>12</b>
<b>Figure S8.</b> Heat capacity of $(MA)_2AgInBr_6$	<b>13</b>
<b>Table S1.</b> A survey of experiments	<b>14</b>
<b>Table S2.</b> Reactions involved in the formation of $(MA)_2AgInBr_6$	<b>15</b>
<b>Table S3.</b> Crystallographic data	<b>16</b>
<b>Table S4.</b> Hydrogen-bond geometry for $(MA)_2AgInBr_6$ at 95K	<b>17</b>
<b>Table S5.</b> Hydrogen-bond geometry for $(MA)_2AgInBr_6$ at 295K	<b>17</b>

## Synthesis.

The starting material, MABr, was prepared by mixing stoichiometric amounts of methylamine solution (40 wt% in H<sub>2</sub>O, Sigma-Aldrich) and HBr (48 wt % in H<sub>2</sub>O, Sigma-Aldrich) at 0°C, then heating at 60°C to dryness, washing with acetone, and drying overnight under vacuum.

Crystals of MAPbBr<sub>3</sub> starting material was grown by mixing stoichiometric amounts of MABr and PbBr<sub>2</sub> (99.9% Alfa Aesar) in HBr (48% in H<sub>2</sub>O, Sigma-Aldrich) at 100°C, followed by cooling to room temperature.

Single crystals of (MA)<sub>2</sub>AgInBr<sub>6</sub> were grown hydrothermally at 150°C for 1 day by mixing stoichiometric amounts of 0.146 g MABr, 0.122g AgBr (99.9% Alfa Aesar) and 0.231 g InBr<sub>3</sub> (99.9% Alfa Aesar) and additional 0.0625 g (10 mol %) of MAPbBr<sub>3</sub> with 1.00 mL 48 wt % HBr solution in Teflon-lined stainless steel autoclaves, followed by slow cooling at 2°C/h. Crystals were then filtered out and washed with ethanol to separate (MA)<sub>2</sub>AgInBr<sub>6</sub> from MAPbBr<sub>3</sub>. To better understand the role of MAPbBr<sub>3</sub> in this synthesis, a series of additional experiments, where molar ratios of the starting materials and/or the presence (*in situ*, *ex situ*, or different amount) of MAPbBr<sub>3</sub> were changed, were performed (Table S1). At the optimum reaction condition (Exp 7, 9 Table S1), secondary phase is totally absent and (MA)<sub>2</sub>AgInBr<sub>6</sub> was obtained at high yield (80%), indicating this synthesis selectively resulted in the target material (MA)<sub>2</sub>AgInBr<sub>6</sub>.

**Single crystal X-ray diffraction.** All reflection intensities were measured at T = 213(2) K and 90(2) K using a SuperNova diffractometer (equipped with Atlas detector) with Mo-K $\alpha$  radiation ( $\lambda = 0.71073 \text{ \AA}$ ) using the program CrysAlisPro (version 1.171.36.32 Agilent Technologies, 2013). The same program was used to refine the cell dimensions and for data reduction. The

crystal structures were solved with the program SHELXS-2013 and were refined on  $F^2$  with SHELXL-2013.<sup>1</sup> The temperature of the data collection was controlled using the system Cryojet (manufactured by Oxford Instruments) (Table S3).

**Powder X-ray diffraction.** Laboratory powder X-ray diffraction (PXRD) patterns were collected using Cu K $\alpha$  radiation ( $\lambda_{\text{avg}} = 1.5418 \text{ \AA}$ ) on a Bruker D8 Focus diffractometer with LynxEye detector. Rietveld refinements of laboratory PXRD data were carried out using TOPAS (Bruker AXS) to determine the crystal structures.

**Neutron diffraction.** The TOPAZ neutron time-of-flight (TOF) single crystal Laue diffractometer at the Spallation Neutron Source, Oak Ridge National Laboratory was used to locate the MA cations in the crystal structures of  $(\text{MA})_2\text{AgInBr}_6$  at  $T = 295(2) \text{ K}$  and  $95(2) \text{ K}$ . Neutrons with wavelengths in the range of 0.4 to 3.5  $\text{\AA}$  were used for the data collection. Sample orientations were optimized with CrystalPlan<sup>2</sup> to ensure full coverage of the asymmetric unit in reciprocal space and a good redundancy for the low symmetry trigonal  $P\bar{3}$  space group. The integrated raw Bragg intensities were obtained using the 3D ellipsoidal  $Q$ -space integration method.<sup>3</sup> Data reduction including Lorentz, absorption, TOF spectrum, and detector efficiency corrections were carried with the ANVRED3 program. The crystal is twinned by merohedry and the reduced data were transformed accordingly to SHELX<sup>1</sup> in HKLF 5 format as a merohedral twin. The twin laws, i.e., twofold rotation about  $[0\ 0\ 1]$ ,  $[1\ 2\ 0]$  and  $[0\ -1\ 0]$  directions, were determined by the TwinRotMat program in PLATON.<sup>4</sup> The atomic coordinates of the inorganic components were obtained from the X-ray data refinement. The atomic positions of the organic MA cation were determined from the difference Fourier map using neutron data.

**Infrared (IR) spectroscopy.** The Fourier transform infrared spectroscopy (FTIR) spectra were collected in reflectance mode using Thermo Scientific Nicolet iS 10 FTIR spectrometer (spectral resolution  $4\text{ cm}^{-1}$ ) in the range  $4000 - 400\text{ cm}^{-1}$ .

**Ultra-violet visible (UV-Vis) spectroscopy.** UV-Vis data were collected on an Agilent Cary 60 UV-Vis spectrometer over the  $200 - 800\text{ nm}$  spectral range at room temperature.

**Thermogravimetric analysis (TGA) and differential scanning calorimetric (DSC) measurements.** TGA and DSC data were collected on TA Instruments SDT Q600 from  $50 - 700\text{ }^{\circ}\text{C}$  under Ar atmosphere.

**Heat capacity measurements.** Heat capacity was measured on a crystal using the semiadiabatic pulse technique, with three repetitions at each temperature ( $2\text{ K} - 300\text{ K}$ ) in a Physical Property Measurement System (PPMS, Quantum Design).

**Figure S1.** Powder XRD showing  $(\text{CH}_3\text{NH}_3)_2\text{AgInBr}_6$  decomposition into  $(\text{CH}_3\text{NH}_3)_4\text{InBr}_7$  and AgBr after heating in the absence of  $\text{PbBr}_2/(\text{MA})\text{PbBr}_3$ .

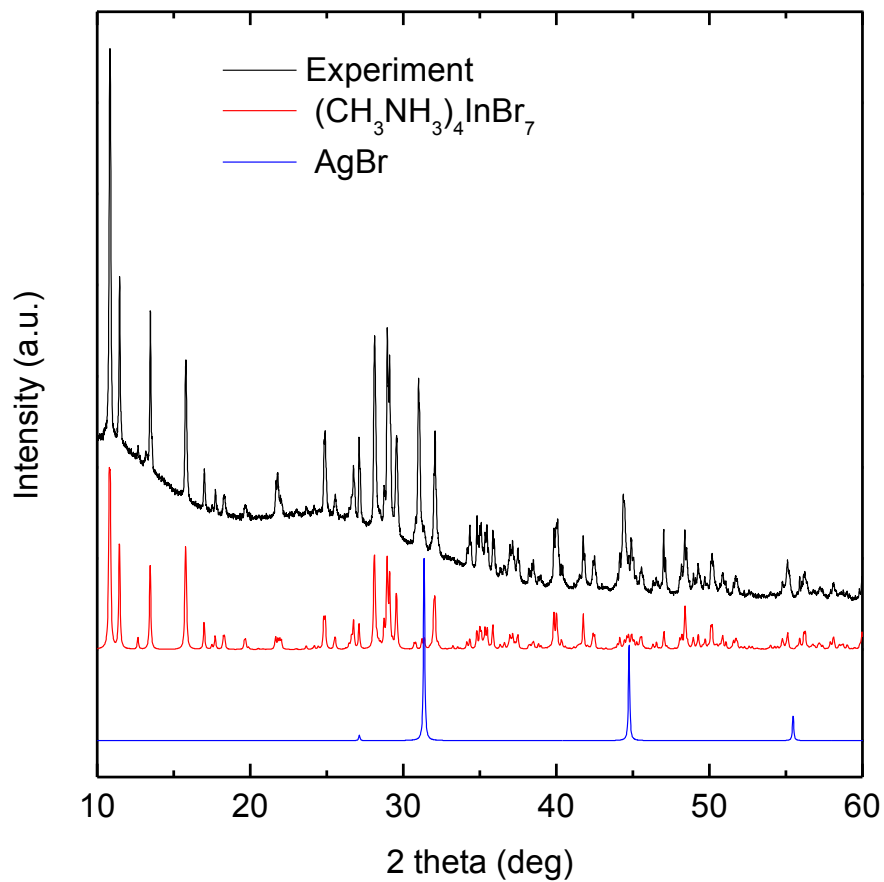


**Figure S2.** Raw spectra used for Jobs analysis for chemical compositions of activated complex.

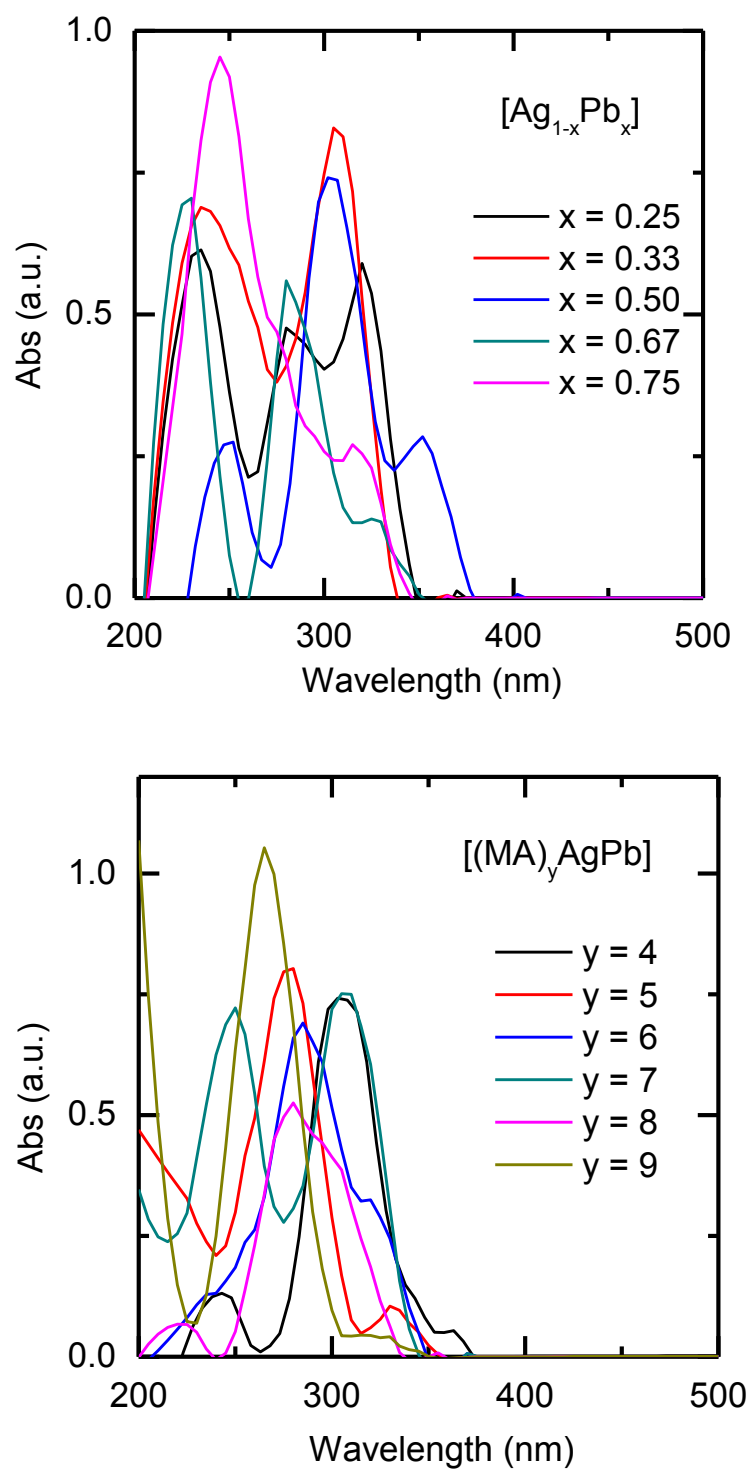


**Figure S3.** Rietveld refinements of the laboratory PXRD pattern of phase-pure  $(\text{CH}_3\text{NH}_3)_2\text{AgInBr}_6$ .

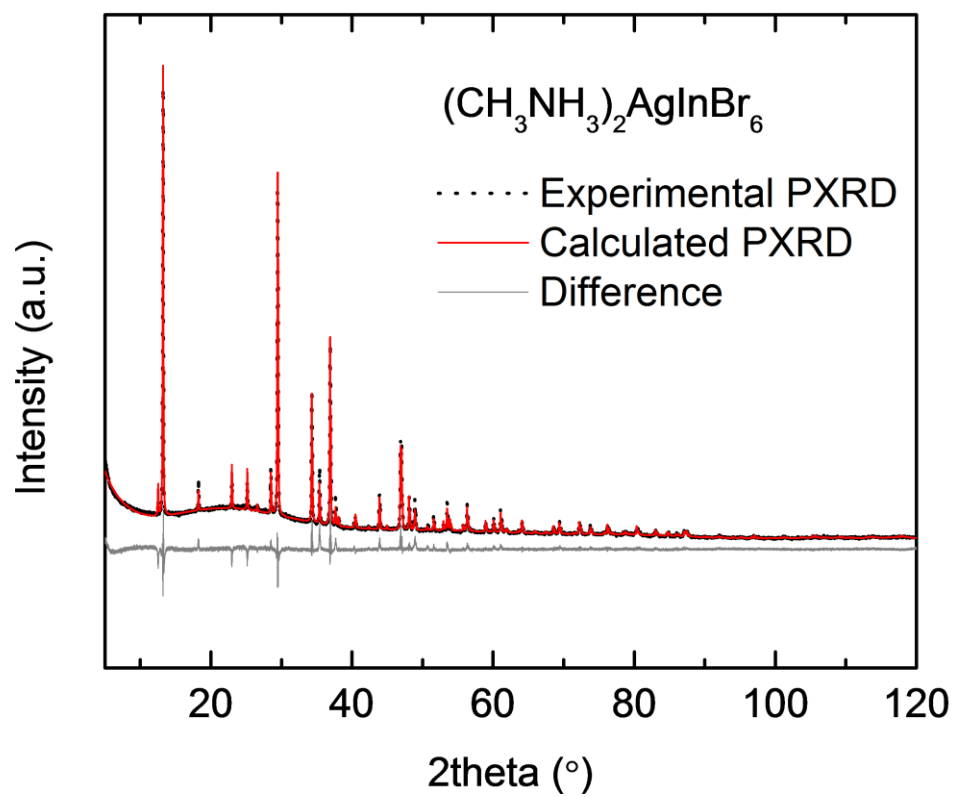




**Figure S4.** IR spectrum of  $(\text{MA})_2\text{AgInBr}_6$ .

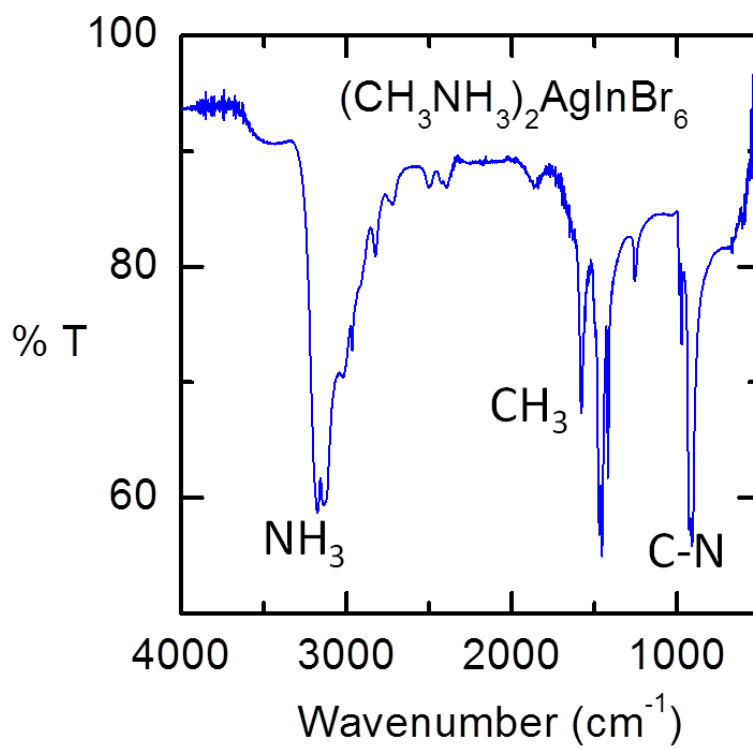


**Figure S5.** UV spectrum of  $(\text{MA})_2\text{AgInBr}_6$ .

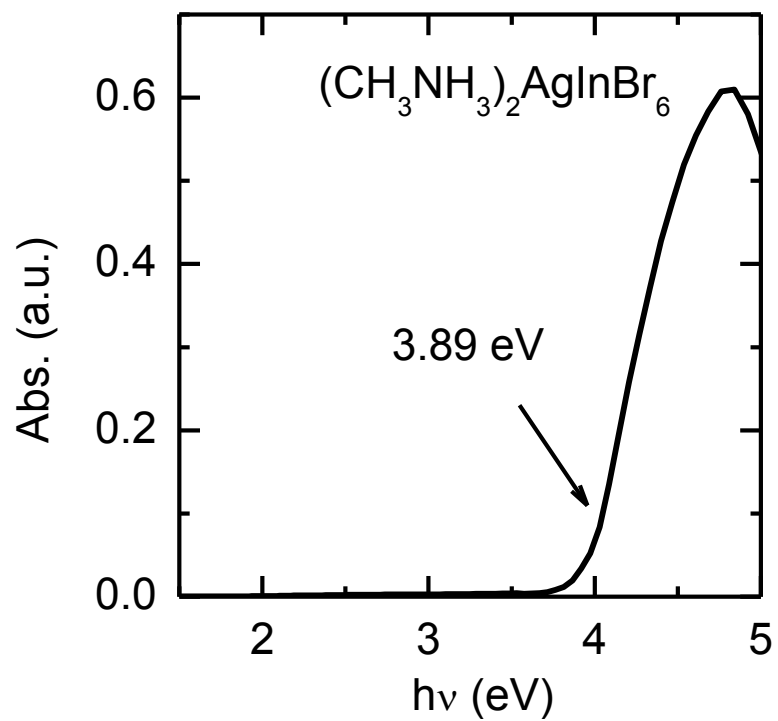


**Figure S6.** TGA and DSC measurements of  $(\text{MA})_2\text{AgInBr}_6$ .

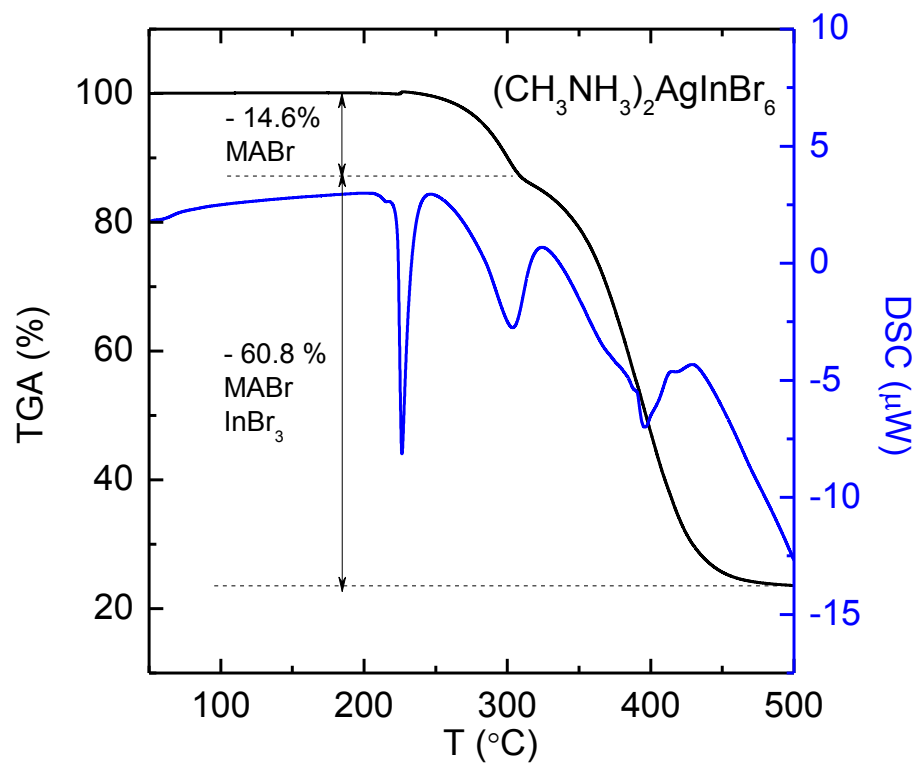


**Figure S7.** PXRD of the residue after the TGA and DSC measurements.

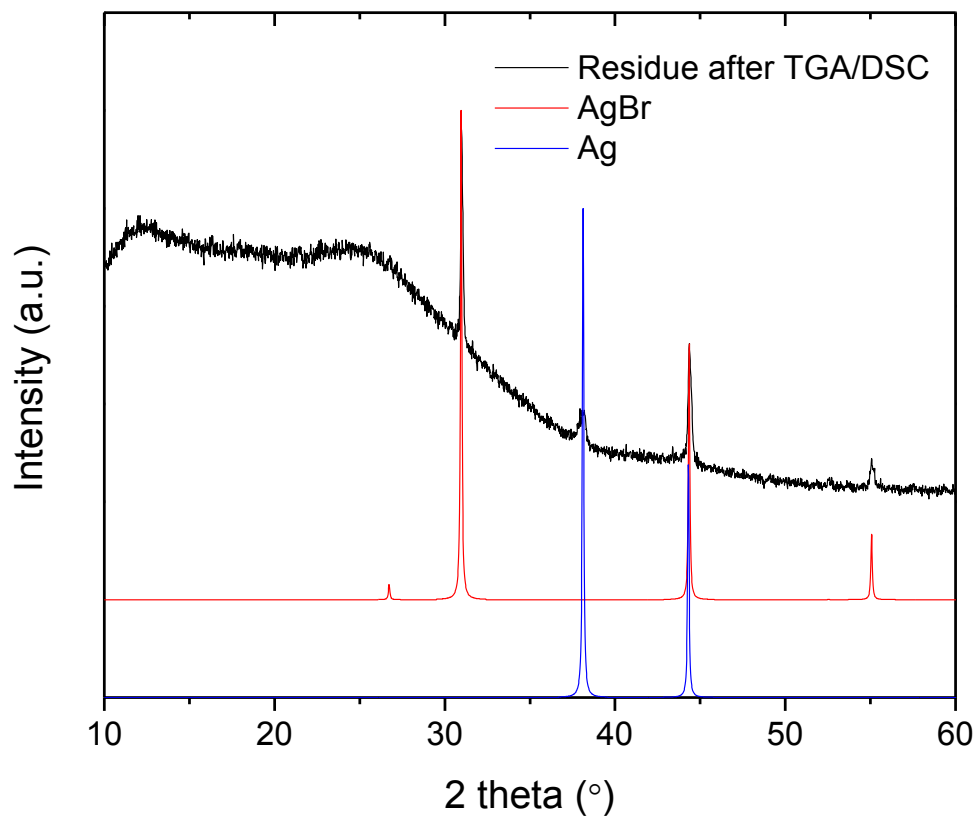


**Figure S8.** Heat capacity of  $(\text{MA})_2\text{AgInBr}_6$ .

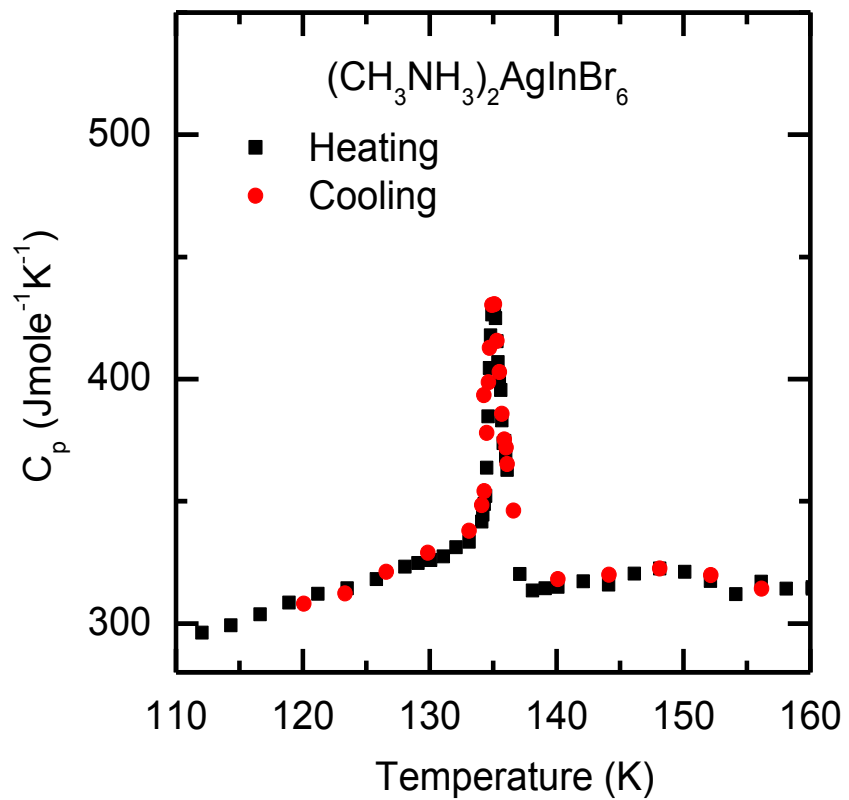


**Table S1.** Results of experiments (at 150°C) with different ratios of starting materials and in the presence (*in situ* or *ex situ*) or absence of PbBr<sub>2</sub>/MAPbBr<sub>3</sub>.

Exp	Starting materials (molar ratios)	Target product		Side products		
		% weight portion	% yield	% weight portion	% yield	
1	AgBr : InBr <sub>3</sub> : MABr	-		(MA) <sub>4</sub> InBr <sub>7</sub>	60%	70%
	1 : 1 : 2			AgBr	40%	90%
2	AgBr : InBr <sub>3</sub> : <b>MABr</b>	(MA) <sub>2</sub> AgInBr <sub>6</sub> 10%	5%	(MA) <sub>4</sub> InBr <sub>7</sub>	30%	60%
	1 : 1 : <b>2.2</b>			AgBr	60%	80%
3	AgBr : InBr <sub>3</sub> : <b>MABr</b>	-		(MA) <sub>4</sub> InBr <sub>7</sub>	60%	80%
	1 : 1 : <b>2.4</b>			AgBr	40%	60%
4	AgBr : InBr <sub>3</sub> : <b>MABr</b>	-		(MA) <sub>4</sub> InBr <sub>7</sub>	70%	85%
	1 : 1 : <b>2.6</b>			AgBr	30%	50%
5	AgBr : InBr <sub>3</sub> : <b>MABr</b>	(MA) <sub>2</sub> AgInBr <sub>6</sub> 15%	10%	AgBr	85%	90%
6	AgBr : InBr <sub>3</sub> : <b>MABr</b>	(MA) <sub>2</sub> AgInBr <sub>6</sub> 10%	5%	AgBr	90%	95%
	1 : 1 : <b>1.6</b>					
7	AgBr : InBr <sub>3</sub> : <b>MABr : PbBr<sub>2</sub></b>	(MA) <sub>2</sub> AgInBr <sub>6</sub> 90%	80%	MAPbBr <sub>3</sub>	10%	70%
8	AgBr : InBr <sub>3</sub> : <b>MABr : PbBr<sub>2</sub></b>	(MA) <sub>2</sub> AgInBr <sub>6</sub> 80%	80%	MAPbBr <sub>3</sub>	20%	80%
	1 : 1 : <b>2.4 : 0.4</b>					
9	AgBr : InBr <sub>3</sub> : <b>MABr : MAPbBr<sub>3</sub></b>	(MA) <sub>2</sub> AgInBr <sub>6</sub> 90%	80%	MAPbBr <sub>3</sub>	10%	70%
10	AgBr : InBr <sub>3</sub> : MABr : <b>(MA)<sub>2</sub>AgInBr<sub>6</sub></b>	(MA) <sub>2</sub> AgInBr <sub>6</sub> 20%	20%	(MA) <sub>4</sub> InBr <sub>7</sub>	40%	80%
	1 : 1 : 2 : <b>0.2</b>			AgBr	40%	70%

**Table S2.** Reactions involved in the formation of  $(MA)_2AgInBr_6$ .

Reaction	Reaction quotient Q
$(MA)_2AgInBr_{6(s)} \leftrightarrow 2MA^+_{(aq)} + [Ag^+_{(aq)}]^* + In^{3+}_{(aq)} + 6Br^-_{(aq)}$	$Q_1 = [MA^+]^2[Ag^+][In^{3+}][Br^-]^6$ (1)
$(MA)_4InBr_{7(s)} \leftrightarrow 4MA^+_{(aq)} + In^{3+}_{(aq)} + 7Br^-_{(aq)}$	$Q_2 = [MA^+]^4[In^{3+}][Br^-]^7$ (2)
$AgBr_{(s)} + 4MA^+_{(aq)} + 4Br^-_{(aq)} \leftrightarrow (MA)_4AgBr_{5(aq)}$	$Q_3 = \frac{[(MA)_4AgBr_5]}{[MA^+]^4[Br^-]^4}$ (3)
$(MA)_4AgBr_{5(aq)} + Pb^{2+}_{(aq)} + 2MA^+_{(aq)} + 4Br^-_{(aq)} \leftrightarrow [(MA)_6AgPb]Br_{9(aq)}$	$Q_4 = \frac{[(MA)_6AgPb]Br_9}{[(MA)_4AgBr_5][Pb^{2+}][MA^+]^2[Br^-]^4}$ (4)
$MAPbBr_{3(s)} \leftrightarrow MA^+_{(aq)} + Pb^{2+}_{(aq)} + 3Br^-_{(aq)}$	$Q_4 = [MA^+][Pb^{2+}][Br^-]^3$ (5)

---

$[Ag^+_{(aq)}]^* = [(MA)_4AgBr_{5(aq)}] + [(MA)_6AgPbBr_{9(aq)}]$

**Table S3.** Crystallographic data for the high temperature (HT) and low temperature (LT) structures of (MA)<sub>2</sub>AgInBr<sub>6</sub> from single crystal X-ray and neutron time-of-flight (TOF) diffraction.

	HT-(MA) <sub>2</sub> AgInBr <sub>6</sub>		LT-(MA) <sub>2</sub> AgInBr <sub>6</sub>	
	X-ray	Neutron TOF	X-ray	Neutron TOF
M/gmol <sup>-1</sup>	766.24	766.24	766.24	766.24
T/K	213(2)	295(2)	95(2)	95(2)
Wavelength (Å)	0.71073	0.40 - 3.49	0.71073	0.40 - 3.49
Crystal system	Trigonal	Trigonal	Trigonal	Trigonal
Space group	<i>P</i> $\bar{3}$ <i>m</i> 1 (No. 164)	<i>P</i> $\bar{3}$ <i>m</i> 1 (No. 164)	<i>P</i> $\bar{3}$ (No. 147)	<i>P</i> $\bar{3}$ (No. 147)
<i>a</i> / Å	7.7021(11)	7.7414(5)	7.6399(2)	7.6324(4)
<i>c</i> / Å	7.0724(14)	7.0841(7)	7.0651(2)	7.0554(6)
<i>V</i> / Å <sup>3</sup>	363.34(13)	367.67(6)	357.126(14)	355.94(5)
<i>Z</i>	1	1	1	1
$\rho_0$ /gcm <sup>-3</sup>	3.681	3.641	3.563	3.575
$\mu$ / mm <sup>-1</sup>	19.681	0.8930 + 1.098 $\lambda$	19.730	0.911 + 1.124 $\lambda$
$\theta$ range/°	2.880 - 26.271	7.387 - 78.264	2.883 - 27.316	7.385 - 78.437
No. of reflections	445	2695	541	1241
No. of parameters	26	85	24	42
<i>R</i> <sub>int</sub>	0.072	0.131	0.076	0.050
GOF	1.270	1.041	1.199	1.105
<i>R</i> ( <i>F</i> ) <sup>a</sup>	0.0237	0.0545	0.0246	0.0352
<i>R</i> <sub>w</sub> ( <i>F</i> <sub>o</sub> <sup>2</sup> ) <sup>b</sup>	0.0569	0.1144	0.0576	0.0662

<sup>a</sup>  $R(F) = \frac{\sum ||F_o| - |F_c||}{\sum |F_o|}$ . <sup>b</sup>  $R_w(F_o^2) = [\frac{\sum w(F_o^2 - F_c^2)^2}{\sum w(F_o^2)^2}]^{1/2}$



<i>D—H···A</i>	<i>D—H</i> (Å)	<i>H···A</i> (Å)	<i>D···A</i> (Å)	<i>D—H···A</i> (°)
<b>N1—H1···Br1</b>	1.011(3)	2.805(4)	3.6468(5)	141.0(2)
<b>N1—H1···Br1</b>	1.011(3)	2.760(3)	3.5142(9)	131.7(3)

<i>D—H···A</i>	<i>D—H</i> (Å)	<i>H···A</i> (Å)	<i>D···A</i> (Å)	<i>D—H···A</i> (°)
<b>N1—H11···Br1</b>	1.01(7)	2.81(7)	3.76(8)	156(5)
<b>N1—H12···Br1</b>	1.03(6)	2.75(5)	3.72(3)	156(7)
<b>N1—H13···Br1</b>	1.01(8)	2.76(5)	3.43(5)	125(4)

## References

- (1) Sheldrick, G. M. *Acta Crystallogr C Struct Chem* **2015**, *71*, 3.
- (2) Zikovsky, J.; Peterson, P. F.; Wang, X.-P. P.; Frost, M.; Hoffmann, C. *J. Appl. Crystallogr.* **2011**, *44*, 418.
- (3) Schultz, A. J.; Jorgensen, M. R. V.; Wang, X.; Mikkelsen, R. L.; Mikkelsen, D. J.; Lynch, V. E.; Peterson, P. F.; Green, M. L.; Hoffmann, C. M. *J. Appl. Crystallogr.* **2014**, *47*, 915.
- (4) Spek, A. L. *Acta Crystallogr D Biol Crystallogr* **2009**, *65*, 148.